

# Up-regulation of brain-derived neurotrophic factor in the dorsal root ganglion of the rat bone cancer pain model

Naoto Tomotsuka<sup>1</sup>  
Ryuji Kaku<sup>1</sup>  
Norihiko Obata<sup>1</sup>  
Yoshikazu Matsuoka<sup>1</sup>  
Hirotaka Kanzaki<sup>2</sup>  
Arata Taniguchi<sup>1</sup>  
Noriko Muto<sup>1</sup>  
Hiroki Omiya<sup>1</sup>  
Yoshitaro Itano<sup>1</sup>  
Tadasu Sato<sup>3</sup>  
Hiroyuki Ichikawa<sup>3</sup>  
Satoshi Mizobuchi<sup>1</sup>  
Hiroshi Morimatsu<sup>1</sup>

<sup>1</sup>Department of Anesthesiology and Resuscitology, Okayama University Graduate School of Medicine, Dentistry and Pharmaceutical Sciences, Okayama, Japan; <sup>2</sup>Department of Pharmacy, Okayama University Hospital, Okayama, Japan; <sup>3</sup>Department of Oral and Craniofacial Anatomy, Tohoku University Graduate School of Dentistry, Sendai, Japan

Correspondence: Naoto Tomotsuka  
Department of Anesthesiology and Resuscitology, Okayama University Graduate School of Medicine, Dentistry, and Pharmaceutical Sciences, 2-5-1 Shikata-cho, Kita-ku, Okayama-shi, Okayama-ken 700-8558, Japan  
Tel +81 86 235 7778  
Fax +81 86 235 6984  
Email t-7010@cf7.so-net.ne.jp

**Abstract:** Metastatic bone cancer causes severe pain, but current treatments often provide insufficient pain relief. One of the reasons is that mechanisms underlying bone cancer pain are not solved completely. Our previous studies have shown that brain-derived neurotrophic factor (BDNF), known as a member of the neurotrophic family, is an important molecule in the pathological pain state in some pain models. We hypothesized that expression changes of BDNF may be one of the factors related to bone cancer pain; in this study, we investigated changes of BDNF expression in dorsal root ganglia in a rat bone cancer pain model. As we expected, BDNF mRNA (messenger ribonucleic acid) and protein were significantly increased in L3 dorsal root ganglia after intra-tibial inoculation of MRMT-1 rat breast cancer cells. Among the eleven splice-variants of BDNF mRNA, exon 1–9 variant increased predominantly. Interestingly, the up-regulation of BDNF is localized in small neurons (mostly nociceptive neurons) but not in medium or large neurons (non-nociceptive neurons). Further, expression of nerve growth factor (NGF), which is known as a specific promoter of BDNF exon 1–9 variant, was significantly increased in tibial bone marrow. Our findings suggest that BDNF is a key molecule in bone cancer pain, and NGF-BDNF cascade possibly develops bone cancer pain.

**Keywords:** BDNF, bone cancer pain, chronic pain, nerve growth factor

## Introduction

Pain is one of the most feared and burdensome symptoms experienced by cancer patients. In a recent systematic review, 64% of advanced cancer patients were suffering from severe cancer-related pain.<sup>1</sup> In particular, cancer patients who develop bone metastasis experience significant pain, and drugs such as opioids and non-steroidal anti-inflammatory drugs often provide an insufficient analgesic effect for such severe pain.

Brain-derived neurotrophic factor (BDNF) is a member of the neurotrophic family and plays important roles in survival, differentiation, and synaptic plasticity of neurons.<sup>2</sup> BDNF is also implicated in the development of pathological pain. In the spinal dorsal horn, BDNF modulates pain transduction by several mechanisms, such as downregulation of potassium chloride co-transporter (KCC2) in a partial nerve ligation model<sup>3</sup> and activation of N-methyl-D-aspartate receptor in an L5 spinal nerve ligation model.<sup>4</sup> Between dorsal root ganglion (DRG) neurons, BDNF acts as an autocrine and/or paracrine signal in an inflammatory pain model and enhances release of neurotransmitter such as calcitonin-gene related protein and substance P.<sup>5</sup> BDNF expression is induced by nerve growth factor (NGF) in DRG neurons<sup>6</sup> and by adenosine-5'-triphosphate in spinal microglia.<sup>3</sup> While the mechanism of BDNF

induction is not fully understood in the bone cancer pain model, a recent study demonstrated that BDNF messenger ribonucleic acid (mRNA) expression increased in DRG, and small interfering RNA (siRNA)-mediated BDNF knockdown reduced the behavioral hypersensitivity in the rat bone cancer pain model induced by prostate cancer cell inoculation.<sup>7</sup>

The rat BDNF gene contains eight non-coding exons (exons 1 through 8) and one coding exon (exon 9).<sup>8</sup> These non-coding exons can be spliced to the coding exon to form the following splice variants: exons 1–9, 2a–9, 2b–9, 2c–9, 3–9, 4–9, 5–9, 6–9, 7–9, 8–9, and 9a–9. Expressions of these splice variants are regulated in an age- and organ-dependent manner.<sup>8</sup> This finding would indicate that multiple promoters are regulating transcription of the splice variants in response to diverse environmental conditions. Our previous studies have clearly demonstrated that BDNF mRNA expression in DRG was up-regulated in inflammatory and neuropathic pain models, and the exon 1–9 variant showed the greatest responses in both models.<sup>9</sup> We also reported that BDNF exon 1–9 was induced by NGF stimulation in cultured DRG neurons.<sup>10</sup> These observations indicated that a specific variant of BDNF mRNA, exon 1–9, can be a strong indicator of various pain. We hypothesized that alternative expression of BDNF and NGF-BDNF cascade is also related to bone cancer pain. In this study, to address this issue, we investigated the expression profile of BDNF splice variants in DRGs in rat bone cancer pain model and the relation between NGF and BDNF expression.

## Materials and methods

### Cell culture

MRMT-1 rat breast cancer cells were provided by the Cell Resource Center for Biomedical Research, Tohoku University (Miyagi, Japan). Cells were cultured in RPMI 1640 supplemented with 300 mg/mL L-glutamine, 10% fetal bovine serum, 200 U/mL penicillin, and 200 µg/mL streptomycin, and incubated at 37°C in a humidified atmosphere of 5% CO<sub>2</sub>.

### Animals

All animal procedures were carried out in accordance with the Ethical Guidelines for the Investigation of Experimental Pain in Conscious Animals issued by the International Association for the Study of Pain.<sup>11</sup> The Board of Animal Care and Use Committee of Okayama University Medical School approved this study on 31 March 2010 (OKU-2010103, Chairman Prof M Nishibori).

Male Wistar rats (170–190 g at surgery, total 54 rats; CLEA Japan, Tokyo, Japan) were housed under controlled conditions (12 hours alternating light–dark cycle, food and water ad libitum).

### Surgical procedure

Injection of MRMT-1 cells was performed as described previously.<sup>12</sup> Briefly, all surgical procedures were performed under 1%–2% isoflurane inhalation anesthesia. After the induction of anesthesia, the left leg was shaved, and the skin was disinfected with 70% v/v ethanol. A 1 cm rostral-caudal incision was made in the skin over the top half of the surface of the proximal end of the tibia. A 24-gauge needle was inserted 5 mm below the knee joint into the intramedullary cavity of the tibia. A cell suspension containing  $3 \times 10^3$  MRMT-1 cells in 10 µL of Hank's buffered sterile saline (HBSS) buffer (Sigma-Aldrich, St Louis, MO, USA) was injected into the medullary space of the left tibia with a 10 µL Hamilton syringe (MRMT-1 group). Control animals were injected with the same volume of HBSS buffer only (Sham group). The injection site was sealed with bone wax, and then the wound was closed, and gentamicin sulfate ointment was applied. After the surgery, the rats were placed in a thermo-regulated recovery box until they had regained consciousness, and they were then returned to the home cage.

### Radiological analysis

Roentgenography of the ipsilateral tibia was performed preoperatively and on postoperative days 7 and 14. Radiographs were taken by a Latheta LCT-200 X-ray imaging system (Hitachi Aloka Medical, Mitaka, Tokyo, Japan) under sodium pentobarbital anesthesia (50 mg/kg, intraperitoneally). After the examination, the rats were placed in a thermo-regulated recovery box until they had regained consciousness, and they were then returned to the home cage.

### Behavioral assessment

Pain behavior was assessed by the von Frey test and measurement of hind limb weight-bearing before and 1–14 days after the surgery. Mechanical allodynia was measured as the hind paw withdrawal threshold (PWT) with von Frey filaments (Touch-Test<sup>®</sup> Sensory Evaluator; North Coast Medical, Morgan Hill, CA, USA). The rats were placed individually in a plastic cage (13 × 10 × 15 cm<sup>3</sup>) with an elevated wire mesh bottom, allowing full access to the plantar surfaces of both hind paws. The mechanical stimuli were applied to the medial plantar aspect of each hind paw with one of a series

of nine von Frey filaments (0.4, 0.6, 1.0, 1.4, 2.0, 4.0, 6.0, 8.0, and 15.0 g). Each trial was started with a von Frey force of 2 g for 1–2 seconds. Stimuli were presented at intervals of at least 10 seconds, allowing for apparent resolution of any behavioral responses to previous stimuli. On the basis of the response pattern and the force of the final filament, the 50% PWT was determined by the up–down method of Dixon<sup>13</sup> and calculated using the formula described by Chaplan et al.<sup>14</sup> If the strongest filament did not elicit a response, the PWT was recorded as 15.0 g.

Hind limb weight-bearing was measured by an Incapacitance Tester (Linton Instrumentation, Norfolk, UK) as described by Fernihough et al.<sup>15</sup> The rat was placed in a chamber so that each hind paw was resting on a separate force transducer pad. Each transducer pad recorded a body-weight on each paw four times in 1 second, and the testing duration was set to 3 seconds. Five readings were averaged for each hind paw, and the results were presented as the weight-bearing ratio (ipsilateral/contralateral).

## Quantitative real-time reverse transcription (RT)-polymerase chain reaction (PCR)

After carrying out behavioral assessment, rats were sacrificed by decapitation under deep ether anesthesia 14 days after the surgery. Ipsilateral L3, L4, and L5 DRG were dissected rapidly and dipped immediately in RNAlater (Qiagen Inc., Valencia, CA, USA). Tibial bone marrow was

collected by flushing 100  $\mu$ L of RNAlater in the tibial cavity. Total RNA was isolated and purified from individual DRG, and the bone marrow with RNeasy Lipid Tissue Mini Kit (Qiagen Inc.). In this process, DNase I was used for removal of genomic DNA according to manufacturer's instruction. Removal of genomic DNA was confirmed by PCR of total RNA with BDNF exon 9 primers (no RT control). Then, 1  $\mu$ g of total RNA was reverse-transcribed with the Ready-To-Go T-primed First-Strand Kit (GE Healthcare Life Sciences, Buckinghamshire, UK). cDNA solutions were diluted ten-fold with DNase-free water. Complementary DNA (cDNA) was amplified in a 20  $\mu$ L real-time PCR reaction mixture containing 10  $\mu$ L SYBR Premix Ex Taq (Takara-Bio, Otsu, Japan), 4.2  $\mu$ L DNase-free water, 0.2  $\mu$ M each of forward and reverse primers, and 5  $\mu$ L diluted cDNA solution. The forward primer for each BDNF splice variant was designed from each non-coding exon, and the reverse primer was designed from the coding region in exon 9 (Figure 1). To quantify expression of total BDNF, forward and reverse primers were both designed from exon 9. The sequences of primer sets are shown in Table 1. Quantitative real-time RT-PCR was performed with a LightCycler<sup>®</sup> (Roche Diagnostics Corporation, Indianapolis, IN, USA) with the following amplification conditions: 95°C for 10 seconds followed by 45 cycles of 5 seconds at 95°C and 20 seconds at 60°C. To quantify absolute cDNA copy numbers, standard curves were created by the following method. Each PCR product with the quantitative primers was cloned into

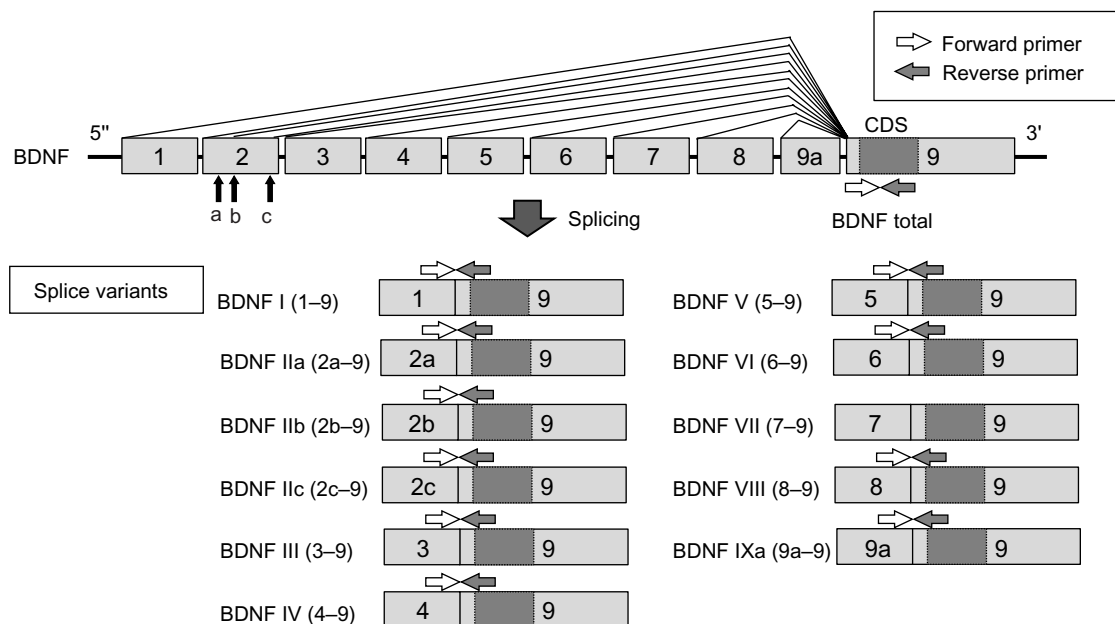


**Figure 1** BDNF gene structure and primer set.

**Abbreviations:** BDNF, brain-derived neurotrophic factor; CDS, coding sequences.

**Table 1** Oligonucleotide sequences of primers for real-time RT-PCR

| Target cDNA | GenBank acc no | Forward primers (5' to 3') | Reverse primers (5' to 3') | Amplicon size (bp) |
|-------------|----------------|----------------------------|----------------------------|--------------------|
| BDNF 1–9    | EF125675       | tggtggggagacgagatatt       | cgtggacgtttgctctcttc       | 159                |
| BDNF 2a–9   | EF125676       | tacttcatccagttccaccag      | caagttgccttgctccgt         | 129                |
| BDNF 2b–9   | EF125677       | aagctccgggtccaccag         | tgcttctttcatgggag          | 102                |
| BDNF 2c–9   | EF125678       | gtgggtgaagccgcaaaga        | cgtggacgtttgctctcttc       | 124                |
| BDNF 3–9    | EF125686       | ctgagactgcgctccactc        | gtggacgtttgctctcttc        | 152                |
| BDNF 4–9    | EF125679       | gagcagctgccttgatgtt        | gtggacgtttgctctcttc        | 148                |
| BDNF 5–9    | EF125687       | accccgacactctgtgta         | acagctgggtaggccaagt        | 204                |
| BDNF 6–9    | EF125680       | gatccgagagctttgtgtgg       | gtggacgtttgctctcttc        | 130                |
| BDNF 8–9    | EF125689       | cagtggagctgaacaaacga       | gccttcacgaaccgaagta        | 117                |
| BDNF 9a–9   | EF125690       | gtctctgcttctctccaca        | cgtggacgtttgctctcttc       | 124                |
| Total BDNF  | NM_012513      | gcggcagataaaaagactgc       | gcagccttcctctgtgtaac       | 141                |
| TrkA        | NM_021589      | ttctcaagtgggagctaggg       | ctctgcctcacgatggaagt       | 155                |
| RPL27       | NM_022514      | gaattgaccctatccaga         | tcgctcctcaaacctgacct       | 200                |

**Notes:** The forward primer for each BDNF splice variant is designed from each non-coding exon. The forward primer for total BDNF is designed from exon 9. All reverse primers except TrkA and RPL27 are designed from exon 9.

**Abbreviations:** BDNF, brain-derived neurotrophic factor; RPL27, 60S ribosomal protein L27; RT-PCR, reverse transcription (RT)-polymerase chain reaction; TrkA, tropomyosin receptor kinase A; bp, base pairs.

pCRII-TOPO (Life Technologies, Carlsbad, CA, USA), and the insert was amplified with M13 forward and reverse primers. The amplified inserts were isolated by agarose gel electrophoresis, extracted from the gel. The concentrations of the oligonucleotides in the gel extracts were measured by spectrophotometry. Absolute copy numbers of the oligonucleotides were calculated from the concentrations and diluted serially to generate standard curves. Expression of each mRNA was normalized to expression of 60S ribosomal protein L27 (RPL27).<sup>16</sup> The data were shown as percentage to mean values of the sham group. PCR specificity was confirmed by sequencing, agarose gel electrophoresis, and melting curve analysis.

### Immunohistochemistry

Rats were anesthetized deeply with ether and perfused transcardially with 50 mL of saline, followed by 500 mL of 4% paraformaldehyde in 0.1 M phosphate buffer (pH 7.4). The L3, L4, and L5 DRG were dissected and post-fixed in the same fixative for 30 minutes, incubated in phosphate-buffered 20% sucrose solution overnight. These tissues were embedded in OCT compound (Tissue-tek®; Sakura Finetek, Tokyo, Japan) and 8 µm thick frozen sections were cut. For visualization of BDNF in the DRG, the avidin-biotin-horseradish peroxidase complex method was used. These sections were incubated overnight with rabbit anti-BDNF antibody (1:4000, #sc-546; Santa Cruz Biotechnology, Santa Cruz, CA, USA), followed by incubation with biotinylated goat anti-rabbit IgG (immunoglobulin G) (1:200) and avidin-biotin-horseradish peroxidase complex (Vector Laboratories, Burlingame,

CA, USA). Immunoreaction products were visualized with diaminobenzidine and nickel ammonium sulfate. DRG neurons were categorized as small (<20 µm diameter), medium (20–40 µm diameter), and large (>40 µm diameter), and the proportion of BDNF-immunoreactive (IR) neurons was analyzed in each group. The cell counting was performed by a blinded observer. Three representative sections that contained over 70 neurons, total at least 210 each neuron, with distinct nuclei were randomly selected in each of the DRG.

### Statistical analysis

Data are presented as means ± standard deviation. The data of hind limb weight-bearing and tactile withdrawal thresholds with von Frey filaments were analyzed by two-way ANOVA (analysis of variance) followed by Scheffe's *F*-test. Data on real-time RT-PCR analysis and the proportion of BDNF-IR neurons were analyzed by Student's *t*-test. *P*<0.05 was considered significant.

## Results

### Osteopenia and pain-related behavior after cancer cell inoculation

Osteopenia caused by growth of inoculated cells was observed in the MRMT-1 group postoperatively (Figure 2A). While osteopenia was gradually increased through day 7–14, cortical integrity was maintained at day 14. This phenomenon represents to clinical observation that bone metastatic cancer cells grow in tibia of a breast cancer patient. It sometimes causes osteolysis. No radiological changes were found in the sham group.

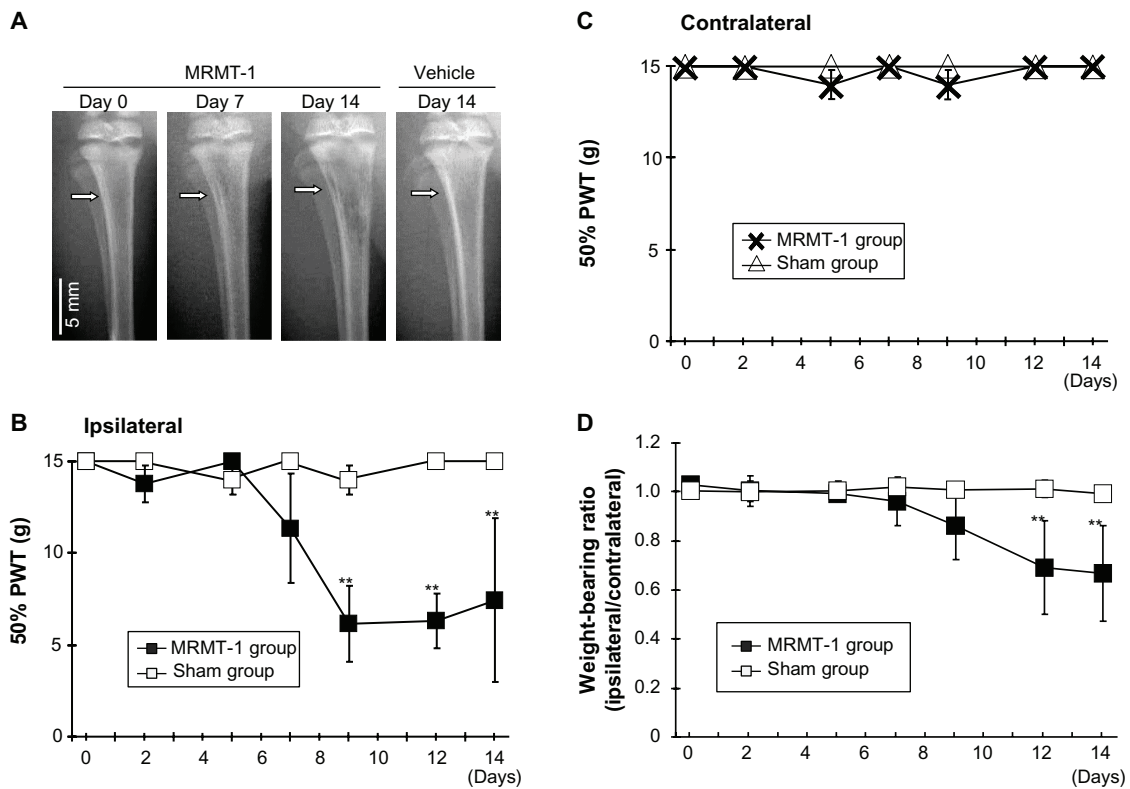


**Figure 2** (A) Radiographs of left tibiae inoculated with MRMT-1 breast cancer cells or vehicle. The white arrow indicates the MRMT-1 injection site. (B) Time course of the ipsilateral PWT to mechanical stimuli after intra-tibial inoculations of Hank's buffered sterile saline (white box,  $n=6$ ) and MRMT-1 cells (black box,  $n=6$ ). These data are reported as means  $\pm$  SD.  $**P<0.01$  versus sham group. (C) Time course of the contralateral PWT to mechanical stimuli after intra-tibial inoculations of Hank's buffered sterile saline (white triangle,  $n=6$ ) and MRMT-1 cells (cross mark,  $n=6$ ). These data are reported as means  $\pm$  SD.  $**P<0.01$  versus sham group. (D) Time course of the hind limb weight-bearing ratio (ipsilateral/contralateral) in rats that received intra-tibial inoculations of Hank's buffered sterile saline (white box) ( $n=6$ ) and MRMT-1 cells (black box) ( $n=6$ ). These data are reported as means  $\pm$  SD.  $**P<0.01$  versus sham group.

**Abbreviations:** PWT, paw withdrawal threshold; SD, standard deviation.

During the observation period, rats with MRMT-1 walked with mild claudication. This observation showed that cancer inoculation did not influence motility nor cause bone fractures at least in the observation period as radiographs also showed. Pain-related behavior was assessed by the von Frey tests (Figure 2B and C) and the hind limb weight-bearing tests (Figure 2D). Prior to intramedullary injection of MRMT-1 or vehicle, there was no difference in ipsilateral 50% PWT between the MRMT-1 group and the sham group. After the injection of MRMT-1, the ipsilateral 50% PWT was decreased significantly on day 9 (MRMT-1 group  $6.2 \pm 2.0$  g versus sham group  $14.8 \pm 0.4$  g,  $P<0.01$ ) (Figure 2B). The decreased 50% PWT was continuously observed until day 14 at the end of the observation period. The contralateral hind limb showed no pain-related behavior in both the MRMT-1 group and sham group during the observation period (Figure 2C). Rats injected with MRMT-1 cells showed significant reduction in weight-bearing on the left hind limb beginning on day 12 (MRMT-1 group  $0.69 \pm 0.19$  versus sham group  $1.01 \pm 0.03$ ,  $P<0.05$ , Figure 2D). These pain-related behaviors progressed

along with the growth of the bone cancer seen in the radiographs (Figure 2A).

## BDNF mRNA and protein was increased in L3 DRG after cancer cell inoculation

Increased BDNF levels in DRG were reported in some pain models and were thought to be involved in pain development. We investigated BDNF expression and localization in DRG neurons. Total BDNF mRNA expression in L3, L4, and L5 DRG are shown in Figure 3A. In the MRMT-1 group, the expression of total BDNF mRNA in L3 DRG increased significantly to 119% compared with the sham group ( $P<0.05$ ). However, no significant differences in the expressions of total BDNF mRNA in the L4 and L5 DRG were seen between the two groups.

To further investigate the expression profiles of BDNF mRNA, expressions of BDNF splice variants were studied. Among all splice variants, exon 1–9 showed the greatest increase, to 207% compared with the sham group ( $P<0.01$ ). Expressions of exons 2a–9, 2b–9, 2c–9, 4–9, and 6–9 also

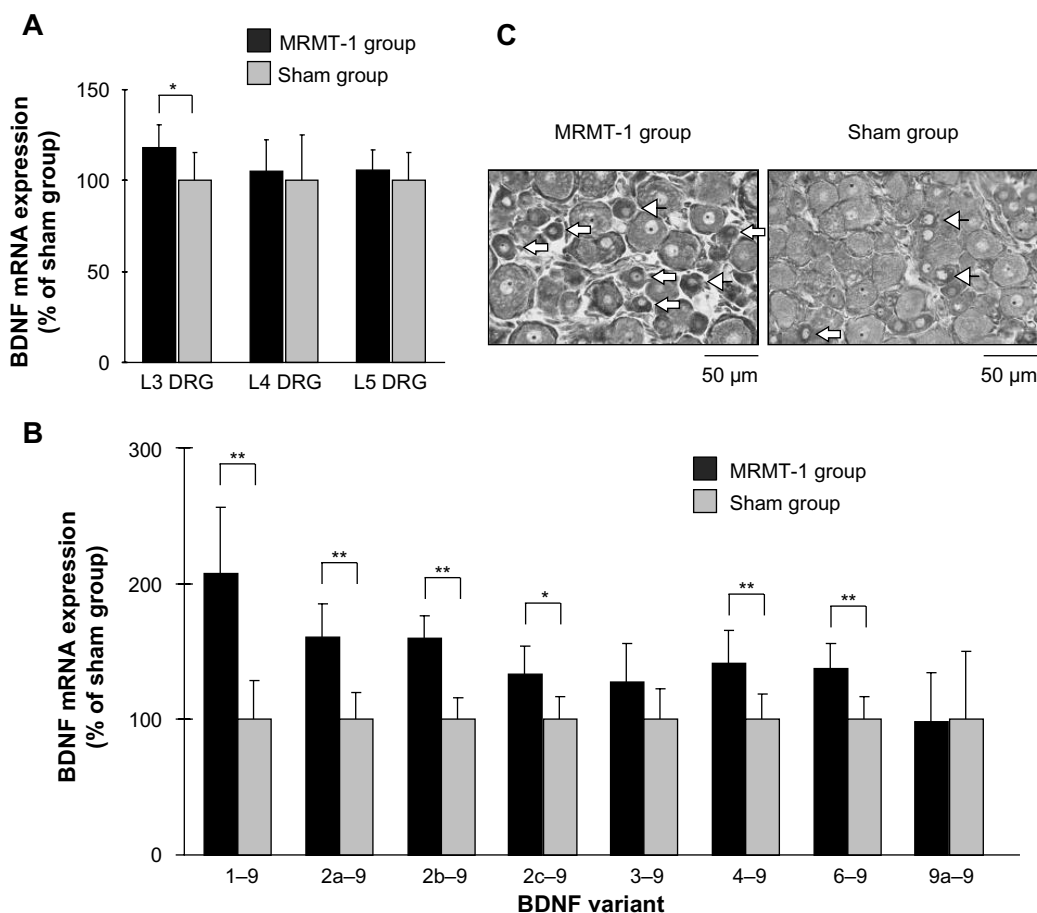


**Figure 3** (A) Relative expression of BDNF mRNA in the ipsilateral L3, L4, and L5 DRG 14 days after MRMT-1 inoculation. These data are shown as percentage to mean values of the sham group. Black bars and gray bars indicate the MRMT-1 groups ( $n=6$ ) and sham groups ( $n=6$ ), respectively. These data are reported as mean  $\pm$  SD.  $*P<0.05$ , versus sham group. (B) Relative expression BDNF splice variants in the ipsilateral L3 DRG 14 days after MRMT-1 inoculation. These data are shown as percentage to mean values of the sham group. Black bars and gray bars indicate MRMT-1 groups ( $n=6$ ) and sham groups ( $n=6$ ), respectively. These data are reported as mean  $\pm$  SD.  $*P<0.05$ ,  $**P<0.01$  versus sham group. (C) Photomicrographs showing the ipsilateral L3 DRG in the MRMT-1 group and sham group 14 days after surgery. Arrows indicate BDNF-positive small sized neurons ( $<20 \mu\text{m}$ ), and arrowheads indicate BDNF-positive medium sized neurons ( $20\text{--}40 \mu\text{m}$ ). **Abbreviations:** BDNF, brain-derived neurotrophic factor; DRG, dorsal root ganglion; mRNA, messenger ribonucleic acid; SD, standard deviation.

increased significantly to 161%, 159%, 133%, 142%, and 137% compared with the sham group, respectively (exon 2c-9,  $P<0.05$ ; other exons,  $P<0.01$ ) (Figure 3B). Expression of exon 3-9 and 9a-9 did not change. Since the absolute copy numbers of exon 5-9 and 8-9 were each below 10 copies/ $\mu\text{L}$ , which was under the lower limit for quantification, data for these exons were excluded from analysis. We could not amplify exon 7-9 in rat neuronal cDNA despite our best efforts. No significant differences in the expressions of BDNF mRNA splice variants in the L4 and L5 DRG were found between the MRMT-1 group and the sham group, as well as in total BDNF mRNA (data not shown).

Figure 3C shows representative photomicrographs of the L3 DRG on day 14. The percentages of BDNF-positive neurons of the left L3, L4, and L5 DRG are shown in Table 2. While the percentage of BDNF-positive neurons in the sham group was similar to a previous report,<sup>17</sup> our new finding

was that BDNF in L3 DRG was significantly increased by MRMT-1 inoculation in only small-sized neurons (136% versus sham group,  $P<0.01$ ) but not in medium- or large-sized neurons (Table 2).

### NGF is one of the key regulators of BDNF in bone cancer pain model

Since BDNF expression in DRG is reported to be induced by systemic administration of NGF,<sup>6</sup> and further BDNF exon 1-9 variant contributes a considerable part of the NGF-induced expression of BDNF mRNA,<sup>10</sup> we investigated NGF expression in the tibial cavity. Quantitative real-time RT-PCR revealed a robust increase of NGF mRNA in the MRMT-1 group (3.8-fold versus sham group,  $P<0.01$ ) (Figure 4).

Since NGF mRNA was increased in the tibial cavity after MRMT-1 inoculation, we investigated

**Table 2** Expression and localization of BDNF in L3, L4, and L5 DRG

| DRG neuron <sup>a</sup> | MRMT-1 group (%) <sup>b</sup> | Sham group (%) <sup>b</sup> | MRMT-1/sham (-fold) | P-value <sup>c</sup> |
|-------------------------|-------------------------------|-----------------------------|---------------------|----------------------|
| <b>L3</b>               |                               |                             |                     |                      |
| Total                   | 15.59±1.42                    | 11.62±0.61                  | 1.34                | 0.0022**             |
| Small                   | 35.89±2.11                    | 26.32±1.66                  | 1.36                | 0.00038**            |
| Medium                  | 13.18±2.45                    | 11.26±1.51                  | 1.17                | 0.23                 |
| Large                   | 3.11±0.99                     | 1.55±1.24                   | 2.00                | 0.23                 |
| <b>L4</b>               |                               |                             |                     |                      |
| Total                   | 13.73±3.79                    | 11.80±2.19                  | 1.16                | 0.41                 |
| Small                   | 30.01±4.77                    | 26.85±1.77                  | 1.11                | 0.26                 |
| Medium                  | 13.52±3.72                    | 11.51±3.46                  | 1.17                | 0.45                 |
| Large                   | 3.56±2.73                     | 3.33±1.75                   | 1.06                | 0.89                 |
| <b>L5</b>               |                               |                             |                     |                      |
| Total                   | 12.73±3.01                    | 9.53±1.26                   | 1.34                | 0.098                |
| Small                   | 26.65±2.14                    | 25.29±2.95                  | 1.05                | 0.48                 |
| Medium                  | 11.59±3.97                    | 8.69±1.27                   | 1.33                | 0.21                 |
| Large                   | 4.11±2.65                     | 2.00±0.84 <sup>a</sup>      | 2.05                | 0.18                 |

**Notes:** <sup>a</sup>DRG neurons were categorized as small (<20 μm), medium (20–40 μm), and large (>40 μm); <sup>b</sup>the data are described as a percentage of BDNF-IR neurons of each group (N=4). The data are reported as mean ± SD; <sup>c</sup>MRMT-1 versus sham group; \*\*P<0.01 versus sham group.

**Abbreviations:** BDNF, brain-derived neurotrophic factor; DRG, dorsal root ganglion; IR, immunoreactive; SD, standard deviation.

expression of NGF receptor, tropomyosin receptor kinase A (TrkA) mRNA in L3 DRG. In the MRMT-1 group, expression of TrkA mRNA was increased significantly to 193% compared with the sham group ( $P<0.01$ , Figure 5).

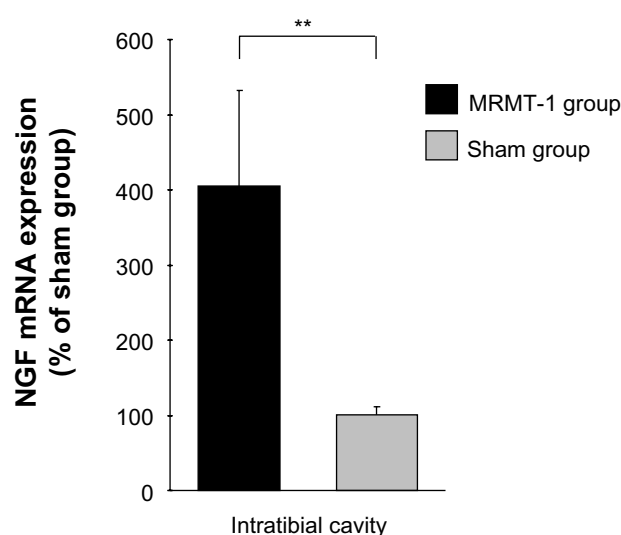


**Figure 4** Relative expression of NGF mRNA in the intra-tibial bone marrow 14 days after MRMT-1 inoculation. These data are shown as percentage to mean values of the sham group. Black bar and gray bar indicate MRMT-1 groups (n=4) and sham groups (n=4), respectively. Expression of each mRNA was normalized to expression of RPL27. These data are reported as mean ± SD. \*\*P<0.01 versus sham group.

**Abbreviations:** NGF, nerve growth factor; mRNA, messenger ribonucleic acid; SD, standard deviation.

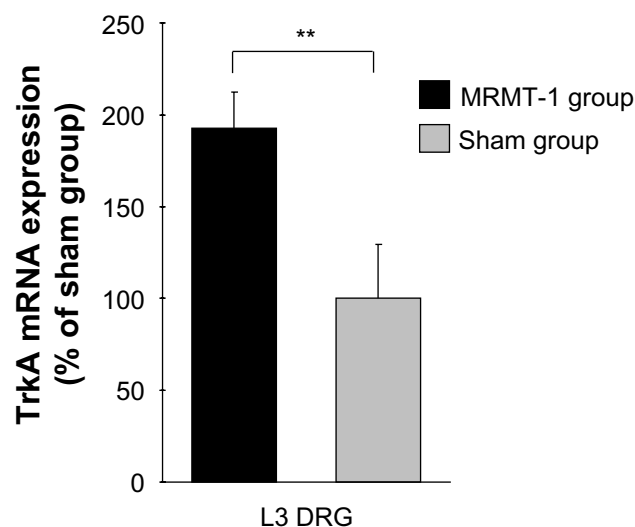


**Figure 5** Relative expression of TrkA mRNA in the ipsilateral L3 DRG 14 days after MRMT-1 inoculation. These data are shown as percentage to mean values of the sham group. Black bars and gray bars indicate the MRMT-1 groups (n=6) and sham groups (n=6), respectively. These data are reported as mean ± SD. \*\*P<0.01, versus sham group.

**Abbreviations:** DRG, dorsal root ganglion; mRNA, messenger ribonucleic acid; TrkA, tropomyosin receptor kinase A; SD, standard deviation.

## Discussion

In this study, we found that inoculation of MRMT-1 cancer cells induced pain-related behavior, and the proportion of BDNF-IR-positive neurons were increased significantly in small neurons in the L3 DRG. Up-regulation of BDNF mRNA in the L3 DRG after MRMT-1 inoculation was observed. Further for detail, among the splice variants, the exon 1–9 variant showed the greatest increase in this model. This report functions as the first report showing the profile of BDNF splice variants in rat bone cancer pain. Expression of NGF, which is known to induce BDNF in DRG neurons, was increased in the intra-tibial cavity with MRMT-1 cells, and its high affinity receptor TrkA was increased in L3 DRG. Our results imply that NGF up-regulation in the tibia play a role in BDNF induction.

The role of BDNF in the development of pathological pain has been well described. BDNF in the spinal dorsal horn modulates synaptic transmission by several mechanisms,<sup>18</sup> including downregulation of KCC2 transporter and conversion of inhibitory GABAergic neurons to excitatory.<sup>3</sup> Although Coull et al<sup>3</sup> regarded spinal microglia as a source of BDNF,<sup>3</sup> anterograde transport of BDNF from DRG sensory neurons contributes to the increase of BDNF in the spinal dorsal horn.<sup>19</sup> BDNF also acts as autocrine and/or paracrine signal between DRG neurons. Up-regulation of BDNF and TrkB receptor were reported in an inflammatory pain model, and BDNF stimulation increased release of neurotransmitter

such as calcitonin-gene related protein and substance P in cultured DRG neurons.<sup>5</sup> Extensive evidence indicates BDNF roles in development of pathological pain in inflammatory<sup>20</sup> and neuropathic<sup>21</sup> pain models. It has also been reported that BDNF mRNA expression was increased in L4–L6 DRG in a rat bone cancer pain model with Walker 256 mammary grand carcinoma cell inoculation.<sup>7</sup> In the present study, we confirmed that BDNF-positive neurons were increased in L3 DRG after MRMT-1 inoculation. Consistently, the report studied by intra-tibial injection of retrograde tracer suggested that tibial bone marrow was innervated mainly by L3 DRG neuron.<sup>22</sup> Taken together with the present study, our novel finding that BDNF-positive neurons were increased in L3 DRG after MRMT-1 inoculation is convincing.

Blockade of BDNF reduces the pain behavior in bone cancer pain,<sup>7</sup> neuropathic pain,<sup>23</sup> and inflammatory pain<sup>24</sup> models. However, suppression of BDNF was documented to result in serious adverse effects, such as early postnatal death in homozygous knockout mouse,<sup>25</sup> decrease or loss of the sensory nervous system in heterozygous knockout mouse,<sup>26</sup> and learning disturbance and memory disorder after the injection of anti-BDNF antibody into the cerebral ventricle.<sup>27</sup> To avoid these effects resulting from systemic blockade of BDNF, local BDNF suppression (eg, intrathecal injection of siRNA,<sup>28</sup> DRG-specific vector transfer mediated by intrathecal injection of AAV8<sup>29</sup>) can be a possible therapeutic tool for pain conditions. We previously reported predominant up-regulation of BDNF exon 1–9 mRNA among the splice variants in L4 and L5 DRG in inflammatory and neuropathic pain models.<sup>9</sup> We also reported that DNA decoy targeting BDNF exon 1 promoter activity showed the anti-nociceptive effect in a rat neuropathic pain model.<sup>30</sup> Since the exon 1–9 variant showed the highest increase in the present study, as well as in other pain models, suppression of BDNF exon 1 transcription might be a therapeutic target for bone cancer pain.

We observed up-regulation of BDNF protein in small neurons in L3 DRG. The majority of small neurons express TrkA, high affinity NGF receptor, and almost all TrkA-positive cells express calcitonin gene-related peptide immunoreactivity.<sup>31</sup> These facts indicate the majority of small neurons are nociceptive and responsive to NGF. On the other hand, most large neurons, which convey proprioception via A-beta fiber, do not express TrkA.<sup>31</sup> Our immunohistochemical results suggest the role of BDNF in cancer-induced bone pain and possible involvement of NGF-TrkA signaling in BDNF up-regulation. Medium to large DRG neurons are reported to change their phenotype and turn to produce

BDNF in pain models accompanying axotomy.<sup>32</sup> We did not observe an increase of BDNF in medium and large neurons in this model.

In the present study, NGF mRNA expression was increased in the intra-tibial cavity in MRMT-1 inoculated rats. In the intra-tibial cavity, MRMT-1 cells are thought to produce NGF. Several lines of evidence on NGF induction of BDNF have been reported. Cultured DRG neurons up-regulate BDNF mRNA in response to NGF stimulation in a dose-dependent manner.<sup>10</sup> We also observed TrkA mRNA expression was increased in the L3 DRG after intra-tibial inoculation of MRMT-1. NGF-TrkA complex is internalized and transported from peripheral terminals to sensory cell bodies in the DRG<sup>33</sup> and activates transcription factors that control downstream gene expression.<sup>33</sup> Systemic administration of NGF to rats induced BDNF mRNA in DRG neurons expressing TrkA receptors.<sup>6</sup> Long-term NGF stimulation induced TrkA mRNA and enhanced intracellular signaling in PC12 cells.<sup>34</sup> Sensory nerve fibers sprouting to bone cancer<sup>35</sup> express TrkA receptor. These findings support the involvement of the NGF-TrkA-BDNF cascade in the present study. Importantly, NGF expression in breast cancer tissue is not limited to experimental conditions. It has been reported that biopsies of human breast cancer showed strong NGF immunoreactivity in most specimens.<sup>36,37</sup>

The limitation of our study is that we do not directly prove involvement of cancer-derived NGF in BDNF induction and pain-related behavior. To clarify the involvement of NGF and BDNF in bone cancer pain, further study is required.

## Disclosure

All authors declare that there is no conflict of interest regarding the publication of this paper.

## References

1. van den Beuken-van Everdingen MH, de Rijke JM, Kessels AG, Schouten HC, van Kleef M, Patijn J. Prevalence of pain in patients with cancer: a systematic review of the past 40 years. *Ann Oncol*. 2007;18:1437–1449.
2. Pezet S, McMahon SB. Neurotrophins: mediators and modulators of pain. *Annu Rev Neurosci*. 2006;29:507–538.
3. Coull JA, Beggs S, Boudreau D, et al. BDNF from microglia causes the shift in neuronal anion gradient underlying neuropathic pain. *Nature*. 2005;438:1017–1021.
4. Geng SJ, Liao FF, Dang WH, et al. Contribution of the spinal cord BDNF to the development of neuropathic pain by activation of the NR2B-containing NMDA receptors in rats with spinal nerve ligation. *Exp Neurol*. 2010;222:256–266.
5. Lin YT, Ro LS, Wang HL, Chen JC. Up-regulation of dorsal root ganglia BDNF and TrkB receptor in inflammatory pain: an in vivo and in vitro study. *J Neuroinflammation*. 2011;8:126.
6. Apfel SC, Wright DE, Wiideman AM, Dormia C, Snider WD, Kessler JA. Nerve growth factor regulates the expression of brain-derived neurotrophic factor mRNA in the peripheral nervous system. *Mol Cell Neurosci*. 1996;7:134–142.



7. Wang LN, Yang JP, Ji FH, et al. Brain-derived neurotrophic factor modulates N-methyl-D-aspartate receptor activation in a rat model of cancer-induced bone pain. *J Neurosci Res*. 2012;90:1249–1260.
8. Aid T, Kazantseva A, Piirsoo M, Palm K, Timmusk T. Mouse and rat BDNF gene structure and expression revisited. *J Neurosci Res*. 2007;85:525–535.
9. Kobayashi H, Yokoyama M, Matsuoka Y, et al. Expression changes of multiple brain-derived neurotrophic factor transcripts in selective spinal nerve ligation model and complete Freund's adjuvant model. *Brain Res*. 2008;1206:13–19.
10. Matsuoka Y, Yokoyama M, Kobayashi H, et al. Expression profiles of BDNF splice variants in cultured DRG neurons stimulated with NGF. *Biochem Biophys Res Commun*. 2007;362:682–688.
11. Zimmermann M. Ethical guidelines for investigations of experimental pain in conscious animals. *Pain*. 1983;16:109–110.
12. Medhurst SJ, Walker K, Bowes M, Kidd BL, et al. A rat model of bone cancer pain. *Pain*. 2002;96:129–140.
13. Dixon WJ. Efficient analysis of experimental observations. *Annu Rev Pharmacol Toxicol*. 1980;20:441–462.
14. Chaplan SR, Bach FW, Pogrel JW, Chung JM, Yaksh TL. Quantitative assessment of tactile allodynia in the rat paw. *J Neurosci Methods*. 1994;53:55–63.
15. Fernihough J, Gentry C, Malcangio M, et al. Pain related behaviour in two models of osteoarthritis in the rat knee. *Pain*. 2004;112:83–93.
16. de Jonge HJ, Fehrmann RS, de Bont ES, et al. Evidence based selection of housekeeping genes. *PLoS One*. 2007;2:e898.
17. Obata K, Yamanaka H, Dai Y, et al. Differential activation of extracellular signal-regulated protein kinase in primary afferent neurons regulates brain-derived neurotrophic factor expression after peripheral inflammation and nerve injury. *J Neurosci*. 2003;23:4117–4126.
18. Merighi A, Salio C, Ghirri A, et al. BDNF as a pain modulator. *Prog Neurobiol*. 2008;85:297–317.
19. Vanelderden P, Rouwette T, Kozicz T, et al. The role of brain-derived neurotrophic factor in different animal models of neuropathic pain. *Eur J Pain*. 2010;14:473. e471–e479.
20. Cho HJ, Kim SY, Park MJ, Kim DS, Kim JK, Chu MY. Expression of mRNA for brain-derived neurotrophic factor in the dorsal root ganglion following peripheral inflammation. *Brain Res*. 1997;749:358–362.
21. Shen H, Chung JM, Chung K. Expression of neurotrophin mRNAs in the dorsal root ganglion after spinal nerve injury. *Brain Res Mol Brain Res*. 1999;64:186–192.
22. Kaan TK, Yip PK, Patel S, et al. Systemic blockade of P2X3 and P2X2/3 receptors attenuates bone cancer pain behaviour in rats. *Brain*. 2010;133:2549–2564.
23. Zhou XF, Deng YS, Xian CJ, Zhong JH. Neurotrophins from dorsal root ganglia trigger allodynia after spinal nerve injury in rats. *Eur J Neurosci*. 2010;12:100–105.
24. Matayoshi S, Jiang N, Katafuchi T, et al. Actions of brain-derived neurotrophic factor on spinal nociceptive transmission during inflammation in the rat. *J Physiol*. 2005;569:685–695.
25. Donovan MJ, Lin MI, Wiegand P, et al. Brain derived neurotrophic factor is an endothelial cell survival factor required for intramyocardial vessel stabilization. *Development*. 2000;127:4531–4540.
26. Ernfors P, Lee KF, Jaenisch R. Mice lacking brain-derived neurotrophic factor develop with sensory deficits. *Nature*. 1994;368:147–150.
27. Mu JS, Li WP, Yao ZB, Zhou XF. Deprivation of endogenous brain-derived neurotrophic factor results in impairment of spatial learning and memory in adult rats. *Brain Res*. 1999;835:259–265.
28. Wang LN, Yang JP, Ji, FH et al. Brain-derived neurotrophic factor modulates N-methyl-D-aspartate receptor activation in a rat model of cancer-induced bone pain. *J Neurosci Res*. 2012;90:1249–1260.
29. Storek B, Reinhardt M, Wang C, et al. Sensory neuron targeting by self-complementary AAV8 via lumbar puncture for chronic pain. *Proc Natl Acad Sci U S A*. 2008;105:1055–1060.
30. Obata N, Mizobuchi S, Itano Y, et al. Decoy strategy targeting the brain-derived neurotrophic factor exon I to attenuate tactile allodynia in the neuropathic pain model of rats. *Biochem Biophys Res Commun*. 2011;408:139–144.
31. Averill S, McMahon SB, Clary DO, Reichardt LF, Priestley JV. Immunocytochemical localization of TrkA receptors in chemically identified subgroups of adult rat sensory neurons. *Eur J Neurosci*. 1995;7:1484–1494.
32. Obata K, Noguchi K. BDNF in sensory neurons and chronic pain. *Neurosci Res*. 2006;55:1–10.
33. Coutaux A, Adam F, Willer JC, Le Bars D. Hyperalgesia and allodynia: peripheral mechanisms. *Joint Bone Spine*. 2005;72:359–371.
34. Zhou J, Valletta JS, Grimes ML, Mobley WC. Multiple levels for regulation of TrkA in PC12 cells by nerve growth factor. *J Neurochem*. 1995;65:1146–1156.
35. Jimenez-Andrade JM, Bloom AP, Stake JI, et al. Pathological sprouting of adult nociceptors in chronic prostate cancer-induced bone pain. *J Neurosci*. 2010;30:14649–14656.
36. Dollé L, El Yazidi-Belkoura I, Adriaenssens E, Nurcombe V, Hondermarck H. Nerve growth factor overexpression and autocrine loop in breast cancer cells. *Oncogene*. 2003;22:5592–5601.
37. Adriaenssens E, Vanhecke E, Saule P, et al. Nerve growth factor is a potential therapeutic target in breast cancer. *Cancer Res*. 2008;68:346–351.